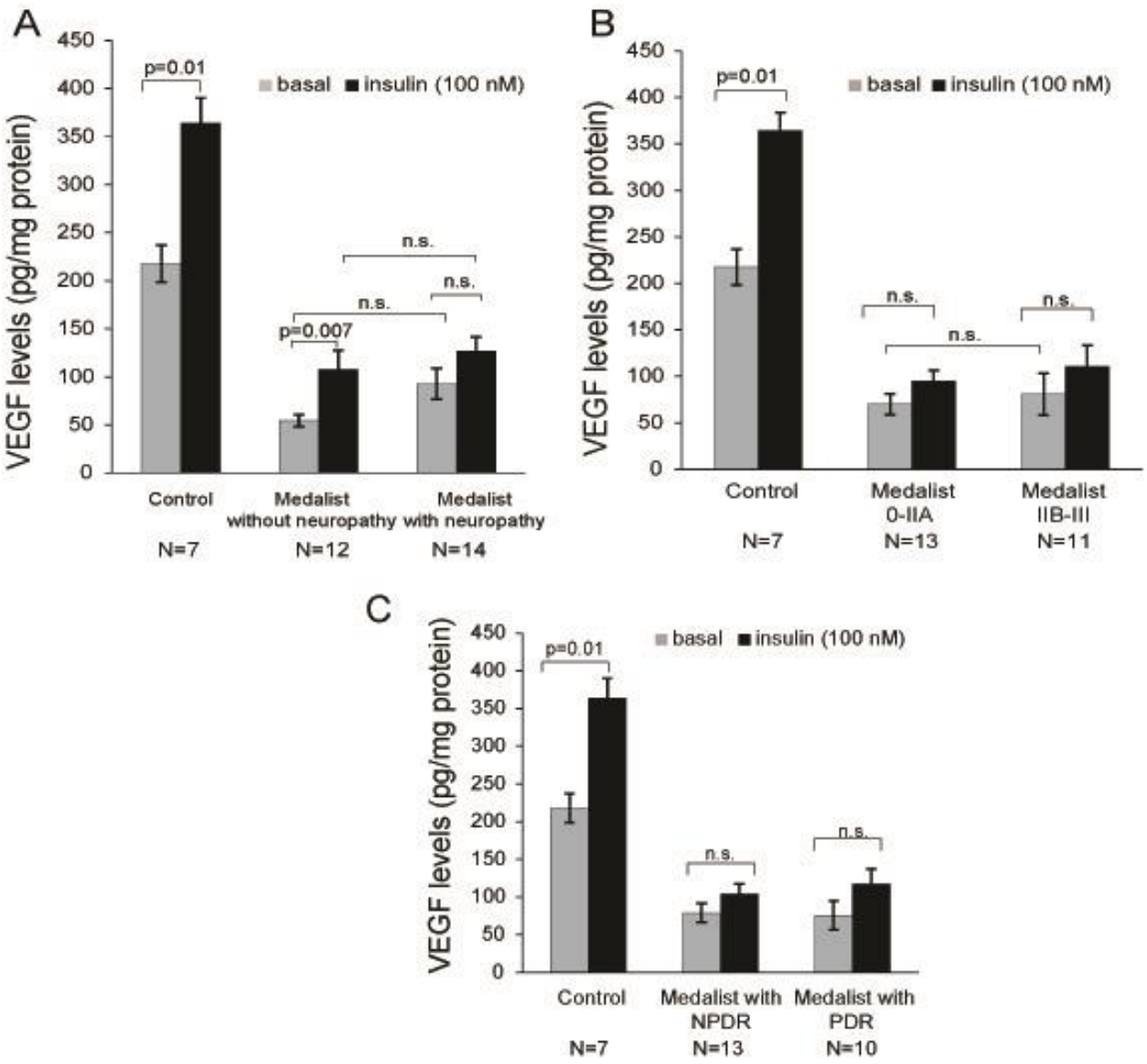

Supplemental figure 1: VEGF protein levels in Medalists with or without neuropathy (**A**), in patients with mild or severe kidney disease (**B**), and in patients with non-proliferative diabetic retinopathy (NPDR) or proliferative diabetic retinopathy (PDR) (**C**), in basal state or after incubation with100 nM insulin for 16 hours. VEGF protein levels secreted to the medium were measured using ELISA kit, each in triplicate. Data presented as mean ± SD obtained from 7 controls and 12 without neuropathy and 12 with neuropathy, 13 with mild kidney disease (0 to 2A) and 11 with severe kidney disease (IIB to III), 13 with NPDR and 10 with PDR. The pathologic classifications for diabetic nephropathy used: Class I, glomerular basement membrane thickening: isolated glomerular basement membrane thickening and only mild, nonspecific changes by light microscopy that do not meet the criteria of classes II through IV. Class II, mesangial expansion, mild (IIA) or severe (IIB): glomeruli classified as mild or severe mesangial expansion but without nodular sclerosis or global glomerulosclerosis in more than 50% of glomeruli. Class III, nodular sclerosis at least one glomerulus with nodular increase in mesangial matrix without changes described in class IV.

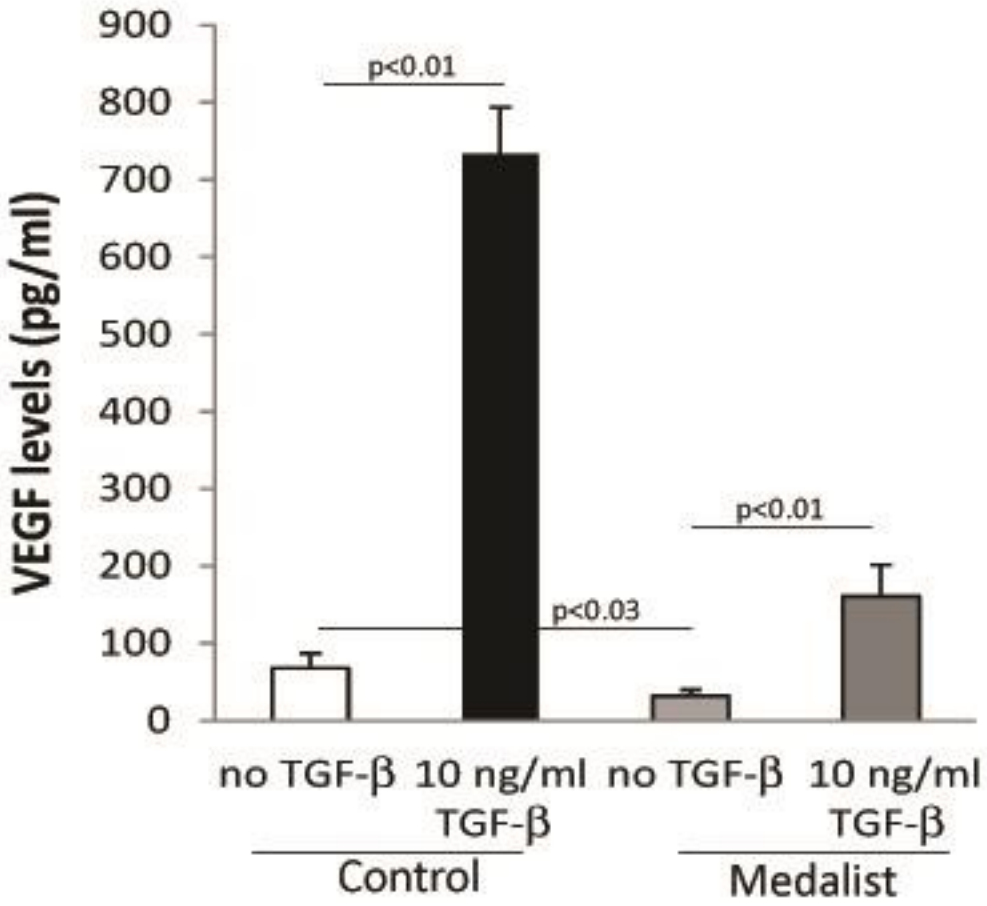

Supplemental Figure 2:
12 hours starved confluent fibroblasts were stimulated with 10 ng/ml TGFβ for 24 hours. VEGF protein levels secreted to the medium were measured using ELISA kit. Data presented as mean ± SD obtained from 6 controls and 6 Medalists, each in triplicate. Student's t-test or chi-square tests were used for two-way comparisons based on the distribution and number of observations of the variable.

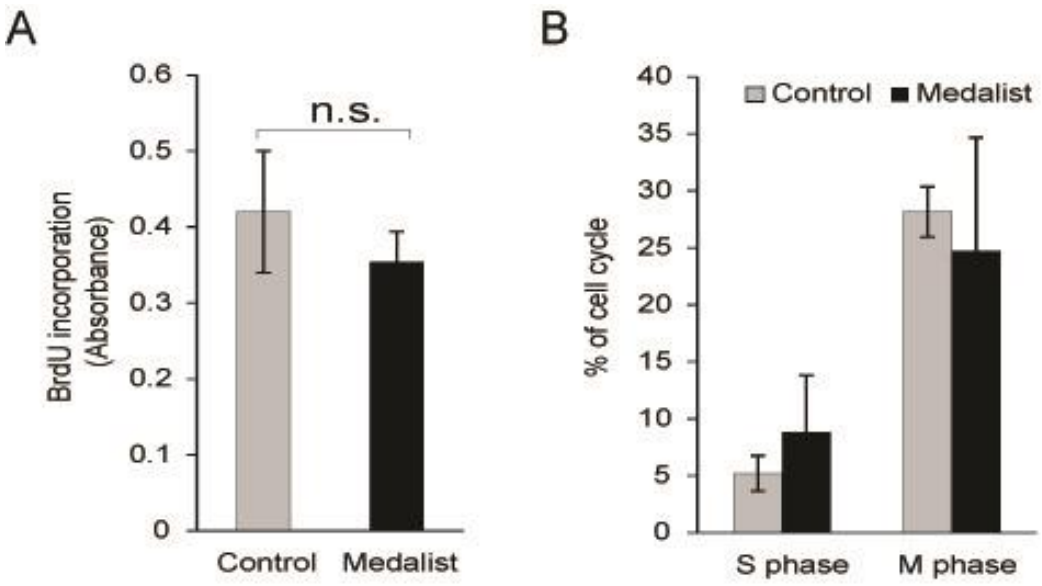

Supplemental Figure 3:
The nucleotide analogue bromodeoxy uridine (BrdU) incorporation into newly synthesized DNA stranded proliferating fibroblasts derived from controls and Medalists is presented in (**A**). Data are mean ± SEM, n= 7 for the control fibroblast group, n= 26 for the Medalist group. (**B**) Following 24 hours fasting, fibroblasts derived from controls and Medalists were incubated with 10% FBS for an additional 24 hours. Cell-cycle distribution was analyzed by flow cytometry. Cells were fixed with 70% ethanol and stained with 50 µg/ml propidium iodide at 37°C for 30 min. Stained cells (1×10^4) were quantified to determine the distribution of different cell cycle phases using Multicycle AV software (FACSAria, BD Biosciences, CA, USA). Data are mean ± SD, n= 7 for the control fibroblast group, n= 10 for the Medalist group.

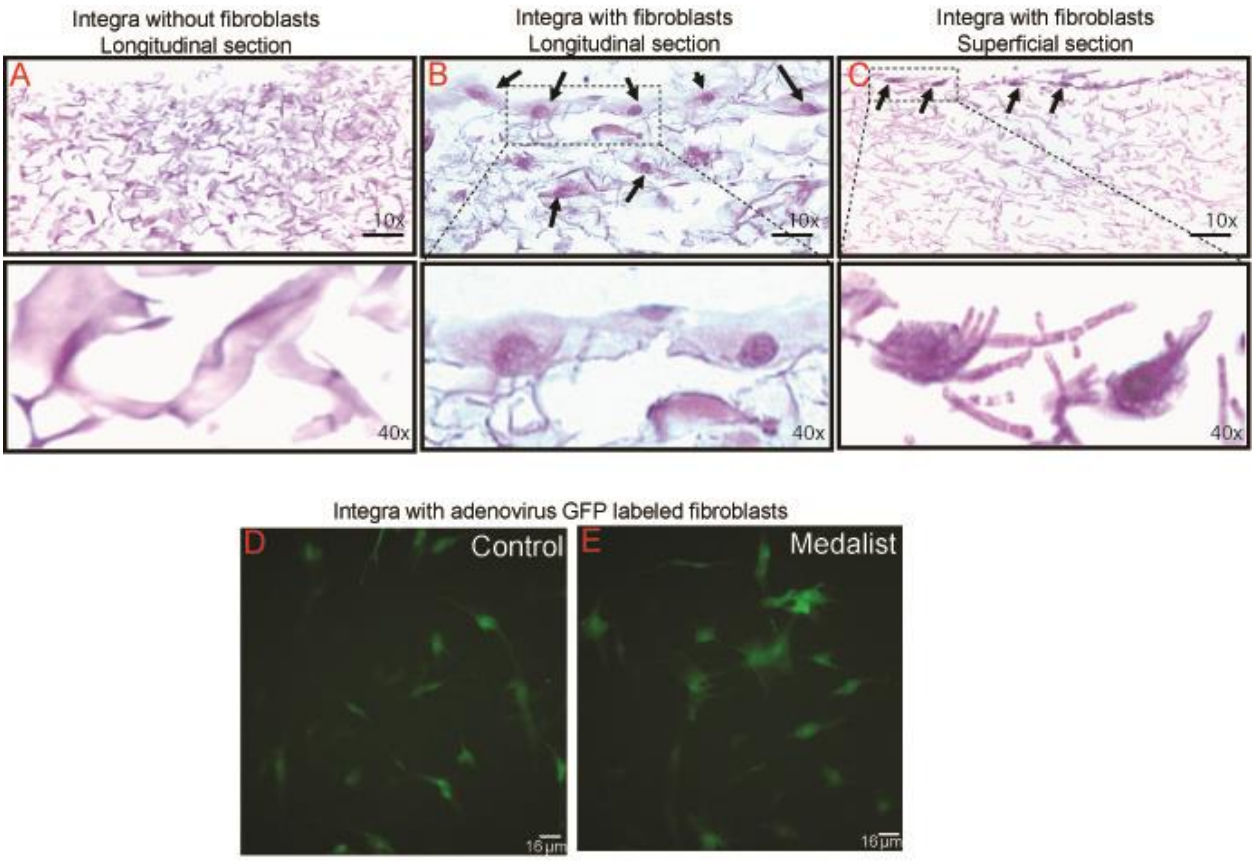

Supplemental Figure 4:
H&E staining for Integra before transplanted. (**A**) Longitudinal section for Integra without fibroblasts. Longitudinal (**B**) and superficial (**C**) sections for Integra seeded with Medalist fibroblasts. GFP labeled fibroblasts from controls (**D**) and Medalists (**E**) on Integra before transplantation.

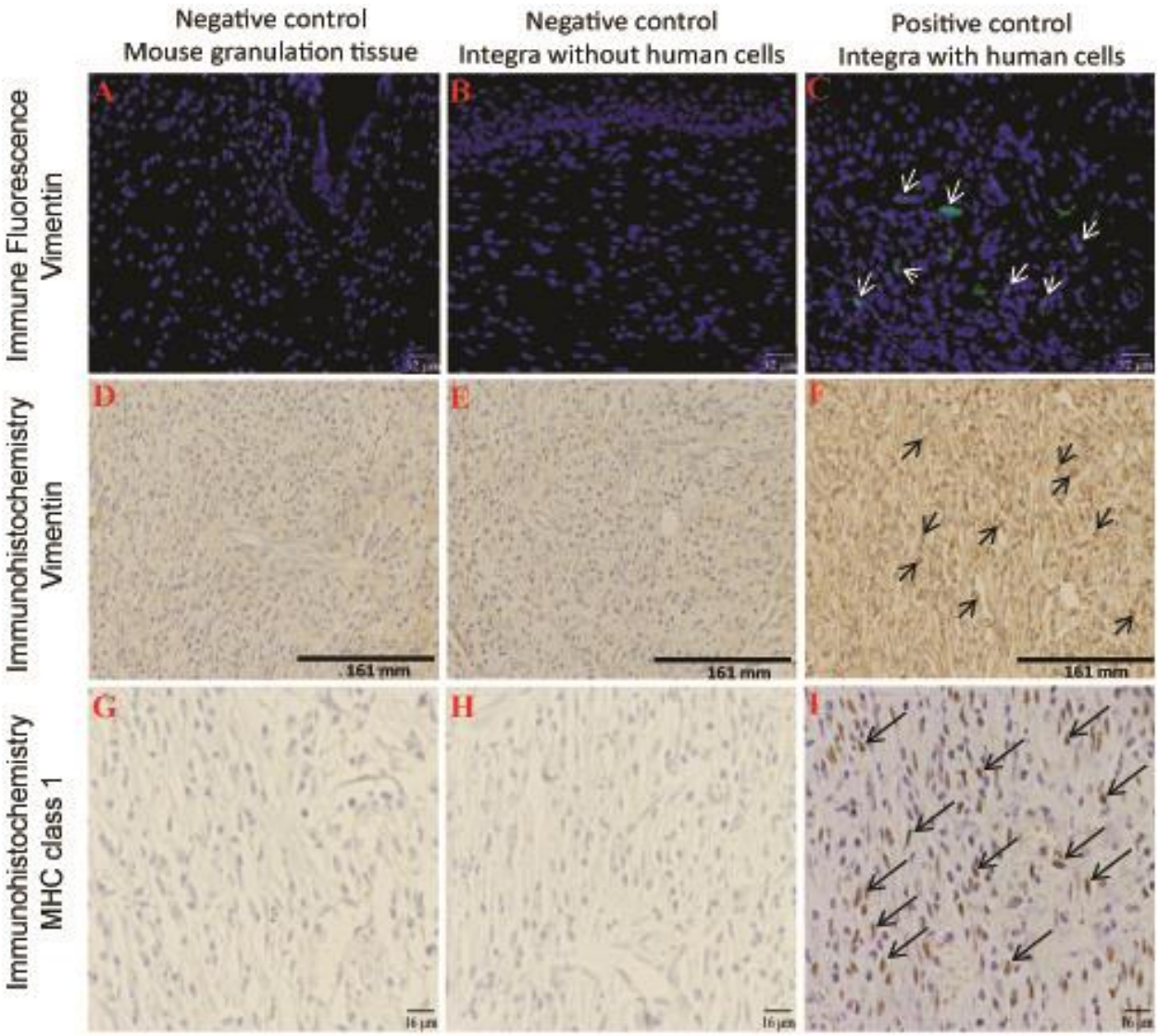

Supplemental Figure 5:
Immune florescence (**A-C**) and immunohistochemistry (**D-F**) for human vimentin expression in mouse granulation tissue obtained from wounds that were not covered with Integra (**A** and **D**), in granulation tissue obtained from wounds transplanted with Integra without human fibroblasts (**B** and **E**), and in granulation tissue obtained from wounds transplanted with Integra seeded with human fibroblasts (**C** and **F**). Green represents human vimentin, and blue represents DAPI. Immunohistochemistry for MHC class 1 in mouse granulation tissue obtained from wounds that were not covered with Integra (**G**), in granulation tissue obtained from wounds transplanted with Integra without human fibroblasts (**H**), and in granulation tissue obtained from wounds transplanted with Integra seeded with human fibroblasts (**I**). n=5 for each treatment group.

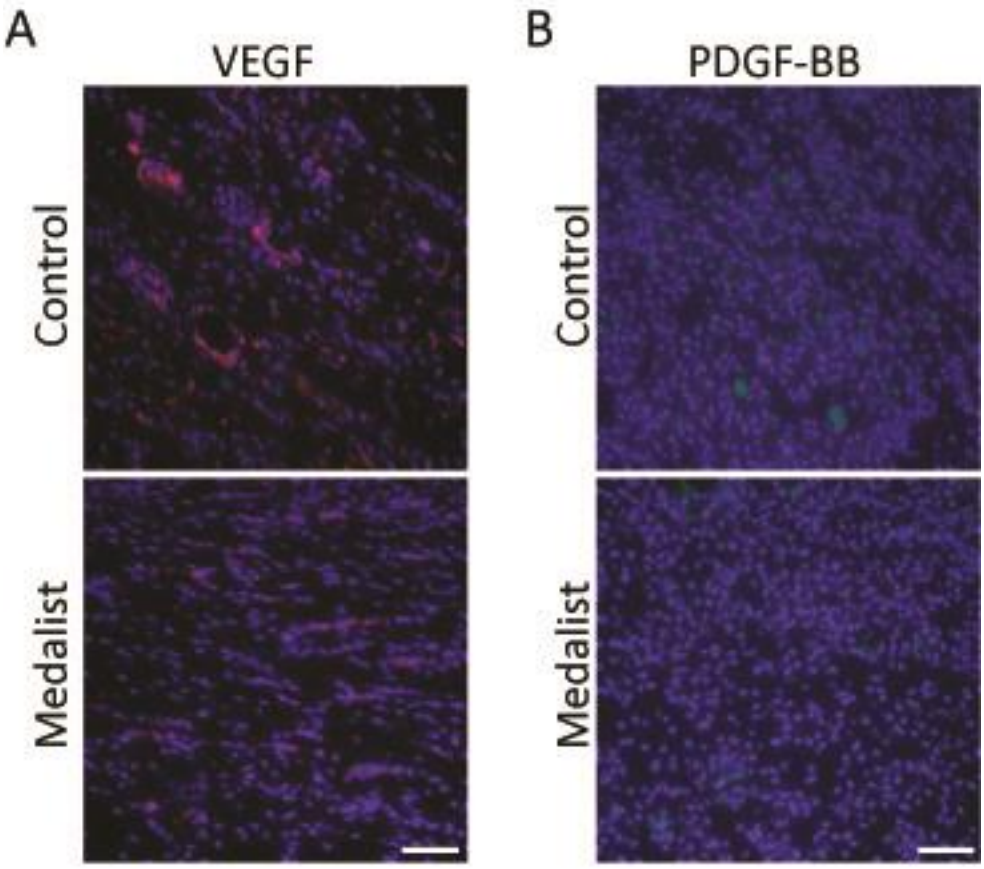

Supplemental Figure 6:
Immunofluorescence for VEGF (**A**) and PDGF-BB (**B**) in granulation tissue obtained from wounds transplanted with Integra seeded with human fibroblasts. Pink represent human VEGF, green represents human PDGF-BB, and blue represents DAPI. n=5 for each treatment group. Scale bar: 50 mm.

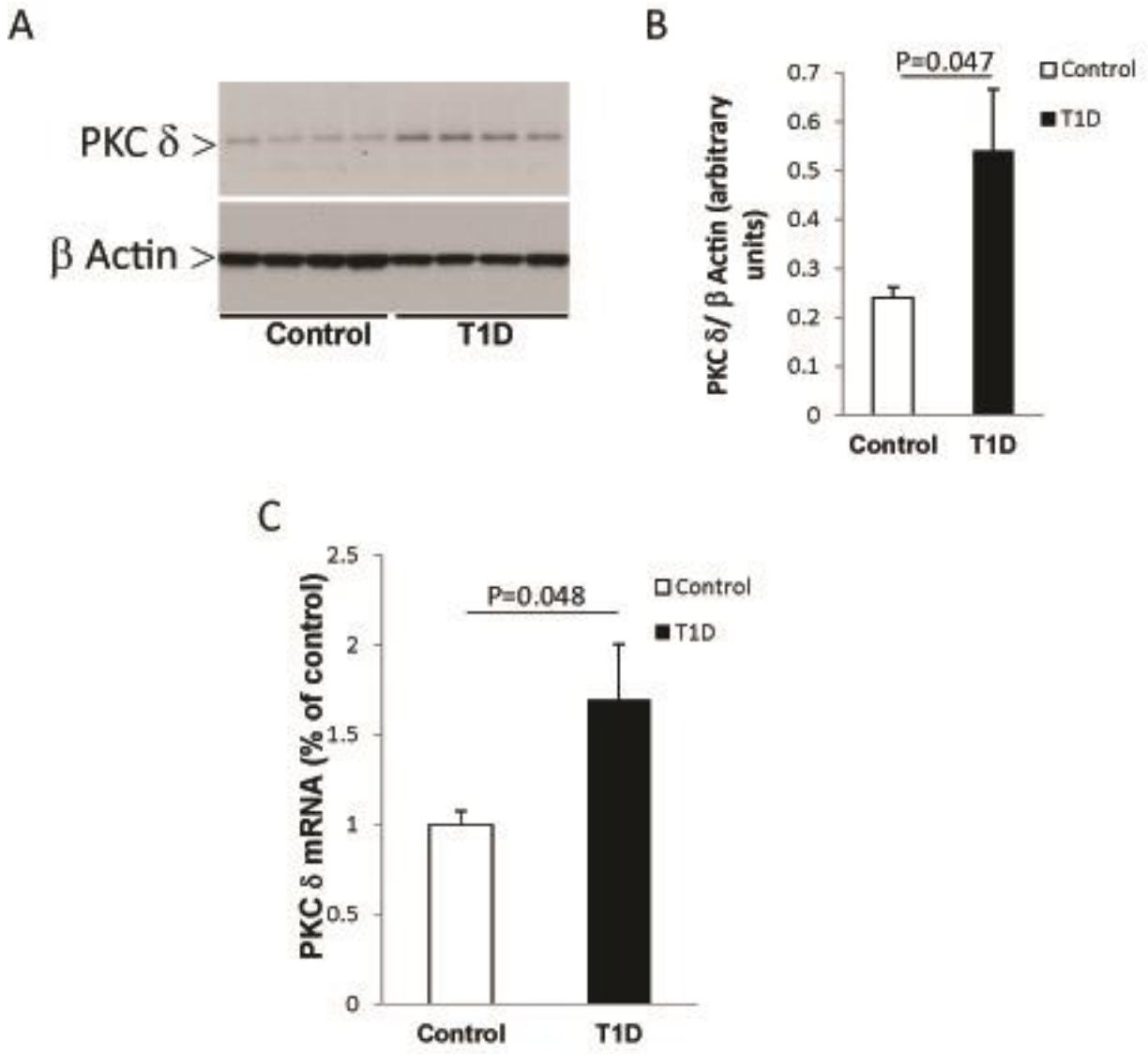

Supplemental Figure 7:
Representative immunoblots for PKCδ protein levels (**A**) and quantification (**B**) and PKCδ mRNA levels (**C**) in fibroblasts derived from skin biopsies obtained from four living type 1 diabetic patients (T1D) and four gender and age matched control healthy non-diabetic donors. Data are mean ± SD. Student's t-test or chi-square tests were used for two-way comparisons based on the distribution and number of observations of the variable.

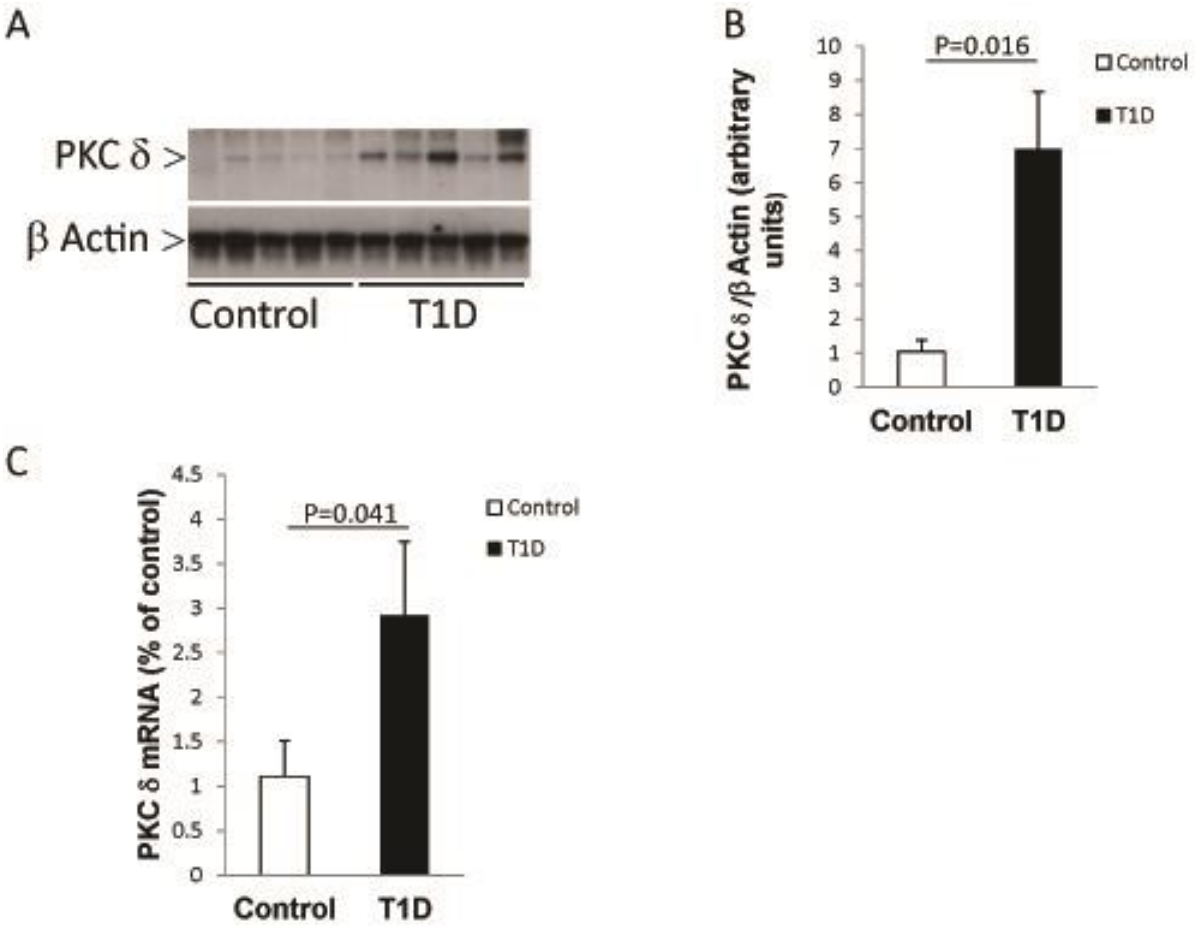

Supplemental Figure 8:
Representative immunoblots for PKCδ protein levels (**A**) and quantification (**B**) and PKCδ mRNA levels (**C**) from living TID patients. The wound samples were obtained from discarded tissues from five active foot ulcers from type 1 diabetic patients and compared to tissues obtained from five gender and age matched non-diabetic patients who had surgery for other indications (eg: hammertoes, bunions and other complications). Data are mean ± SD. Student's t-test or chi-square tests were used for two-way comparisons based on the distribution and number of observations of the variable.

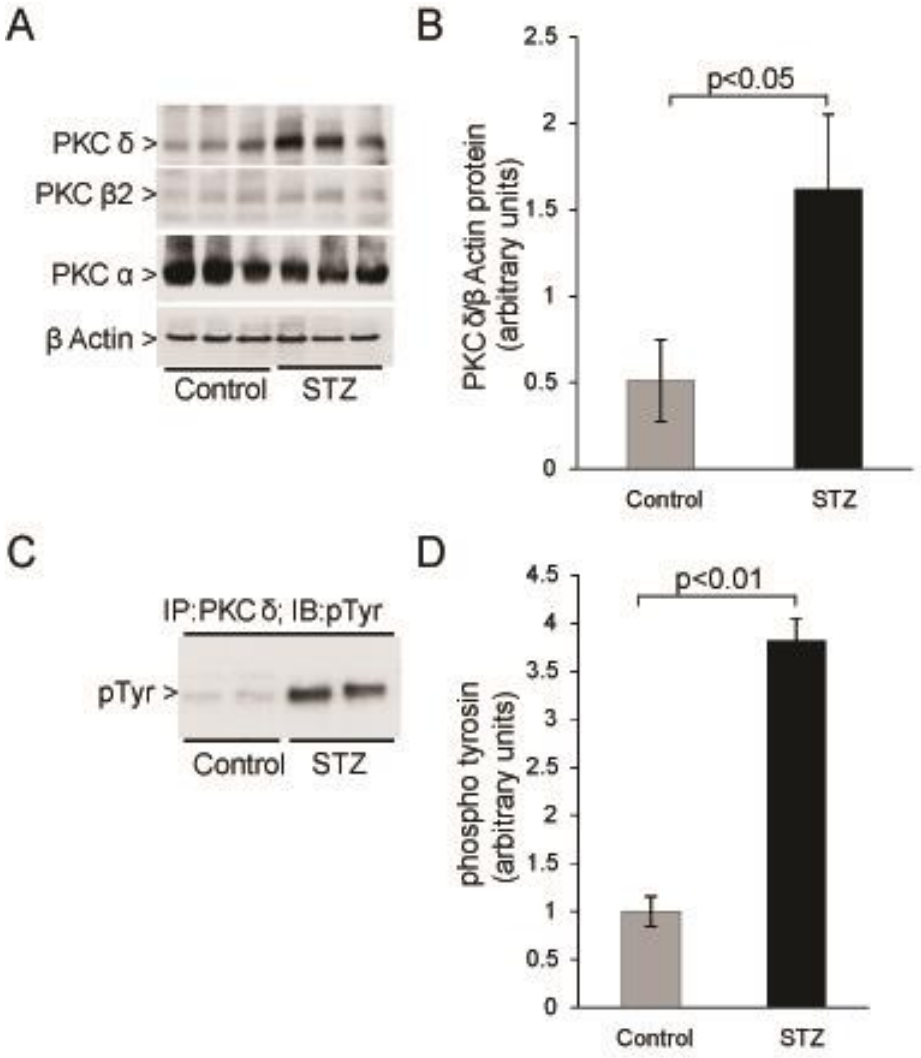

Supplemental Figure 9:
Representative immune-blots for PKCδ, α, and β2 isoforms in granulation tissue obtained 9 days after the initial wounding incision in STZ induced diabetic mice injected with STZ two weeks before wounding (**A**), and (**B**) the quantification of the blots. Representative immunoblots (**C**) and quantification (**D**) for tyrosine phosphorylation on PKCδ in granulation tissues obtained from control and STZ induced diabetic mice, after immunoprecipitation with anti-PKCδ antibody. Data are mean ± SD, n= 5 in each group.

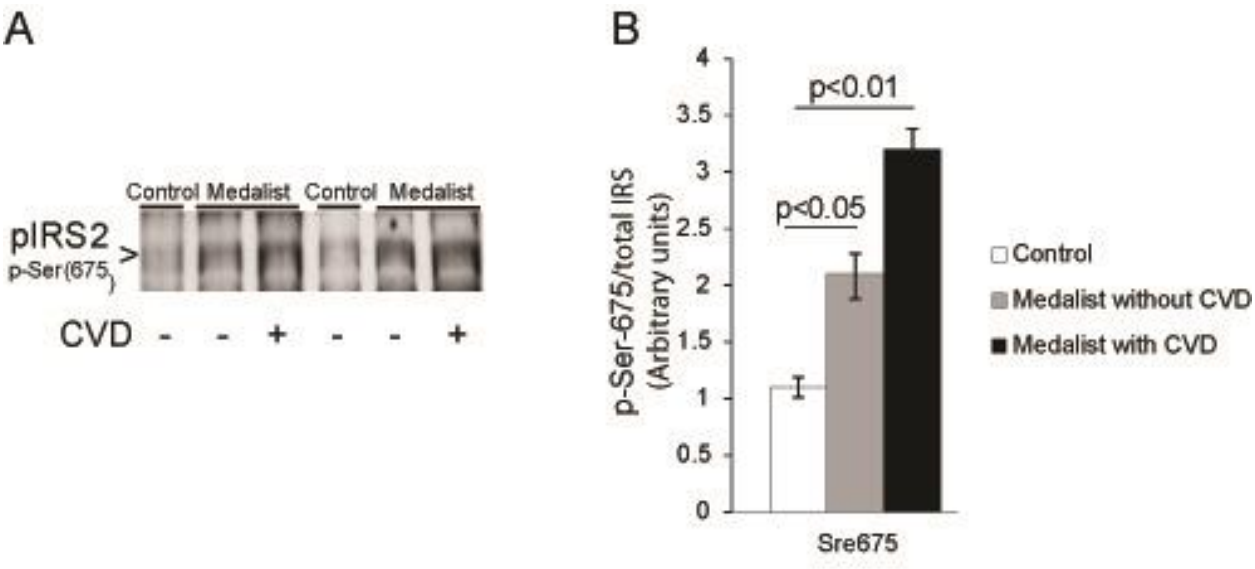

Supplemental Figure 10:
(**A**) Representative immune-blots for p-Ser675 site of IRS2 in fibroblasts derived from control, Medalist without or Medalist with CVD, and the quantifications (**B**) corrected to total IRS2. Data are mean ± SD, n= 7 for the control fibroblast group, n= 8 in each group of Medalists with or without CVD.

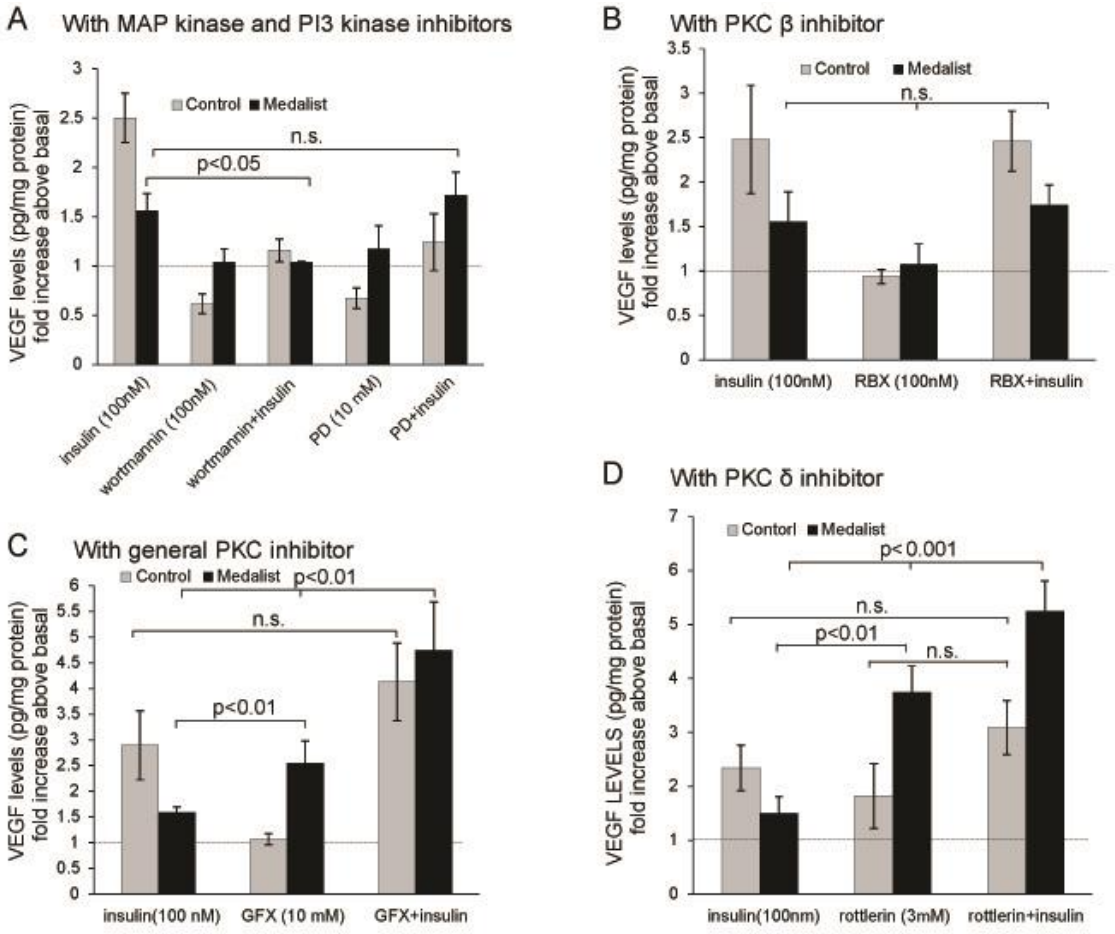

Supplemental Figure 11:

VEGF levels in fibroblasts derived from controls or Medalists incubated with 100 nM insulin in the presence of 100 nM wortmanin (a PI3 kinase), or 10 μM PD98059 (a MAP kinase inhibitor (**A**), or with 100 nM RBX (a general PKCβ) (**B**), or with 10 mM GFX (a general PKC inhibitor) (**C**), or with 3 μM rottlerin (a PKCδ inhibitor) (**D**). Data are mean ± SD, n= 7 for the control fibroblast group, n= 12 in the Medalist group.

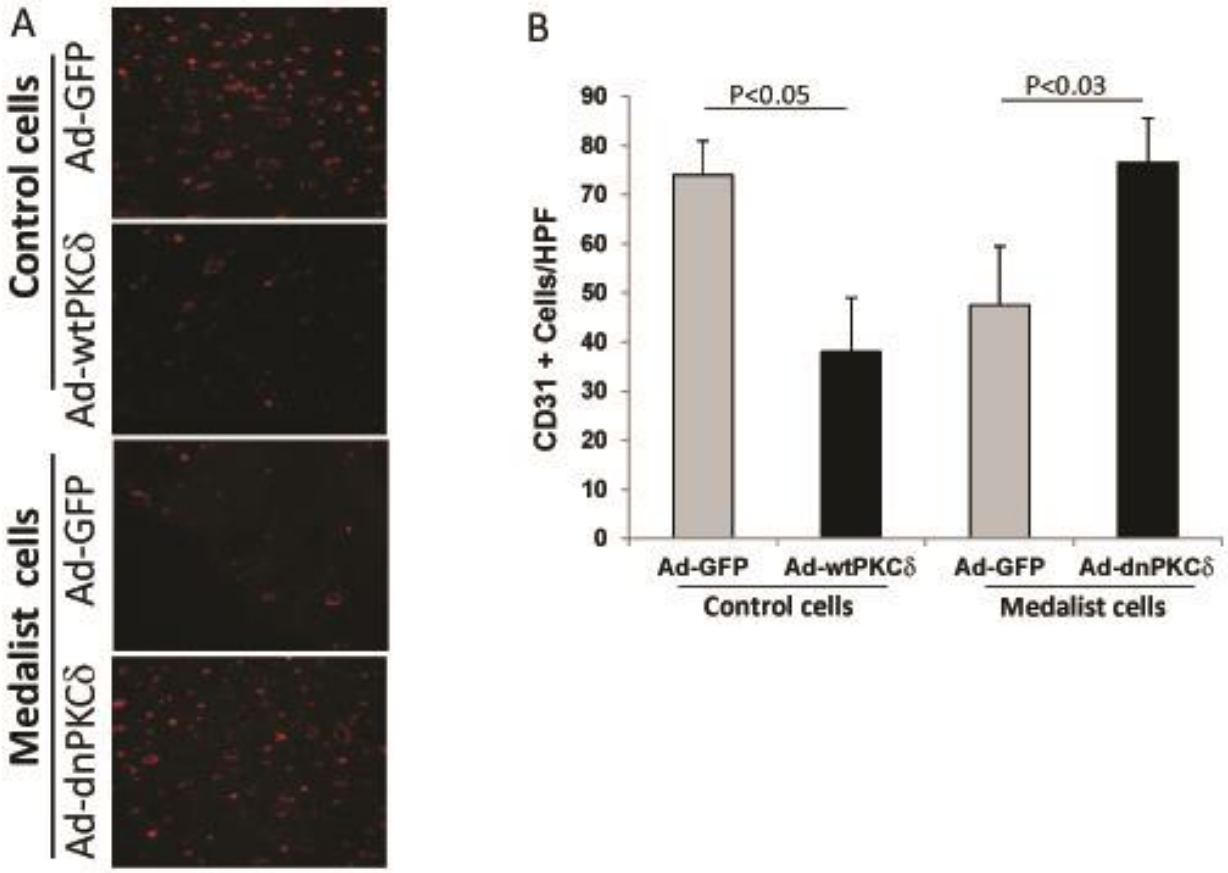

Supplemental Figure 12:
Extent of neovascularization in granulation tissues on day15 post-wounding was assessed by CD31+ positive cells using immunofluorescence (**A**) and quantification (**B**). Data are mean ± SD, n= 7 for the control fibroblast group, n= 8 for Medalists with CVD, and n = 8 for Medalists without CVD. The criteria for selecting the cell lines for these experiments were completely random, and the selected subjects did not differ in any clinical or demographic characteristics from the rest of the patients. Student's t-test or chi-square tests were used for two-way comparisons based on the distribution and number of observations of the variable. Scale bar: 50 mm.

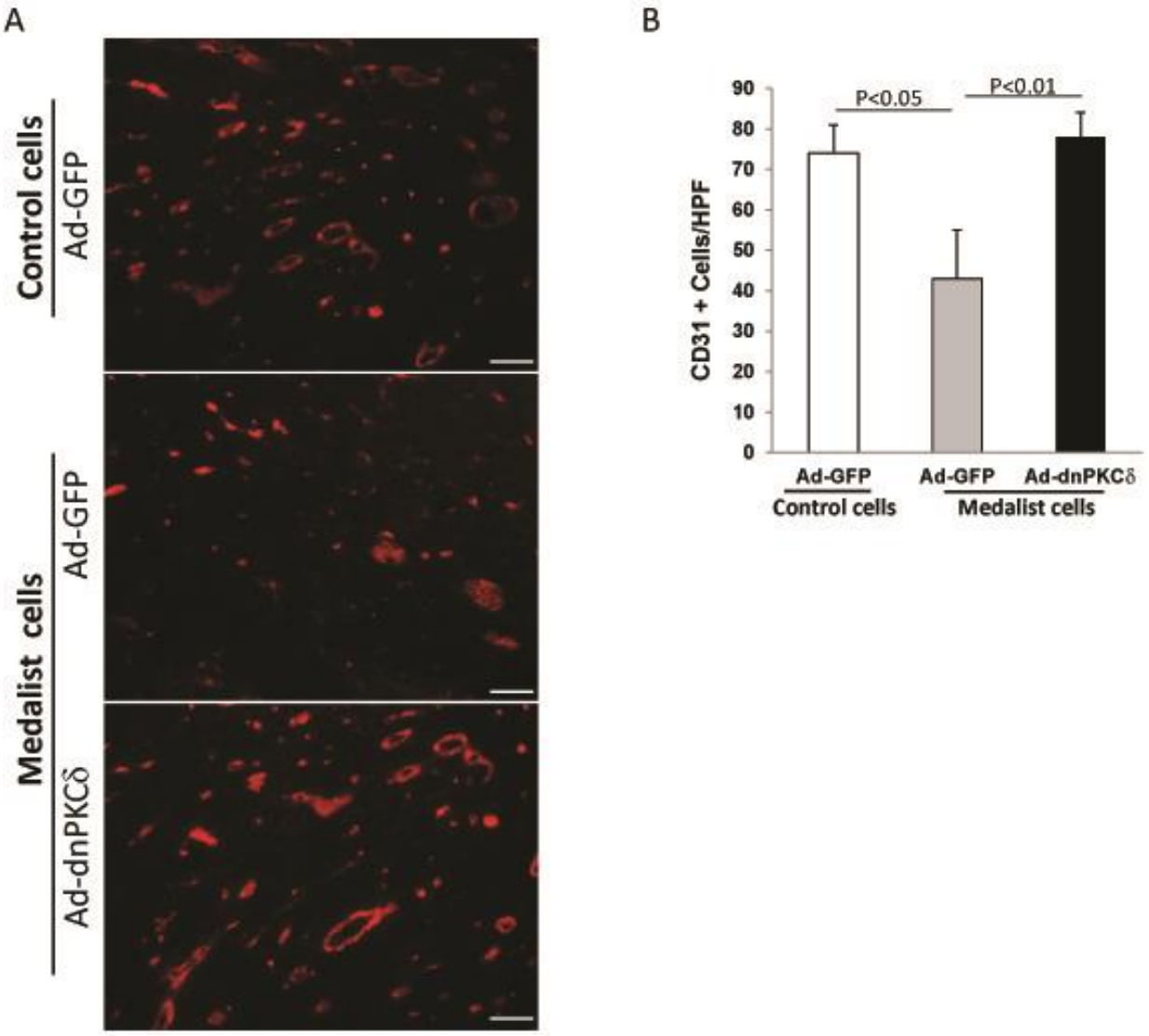

Supplemental Figure 13:
Extent of neovascularization in granulation tissues on day15 post-wounding was assessed by CD31+ positive cells using immunofluorescence (**A**) and quantification (**B**). Data are mean ± SD, n= 7 for the control fibroblast group, n= 8 for the Medalist group. The criteria for selecting the cell lines for these experiments were completely random, and the selected subjects did not differ in any clinical or demographic characteristics from the rest of the patients. Student's t-test or chi-square tests were used for two-way comparisons based on the distribution and number of observations of the variable. Scale bar: 50 mm.

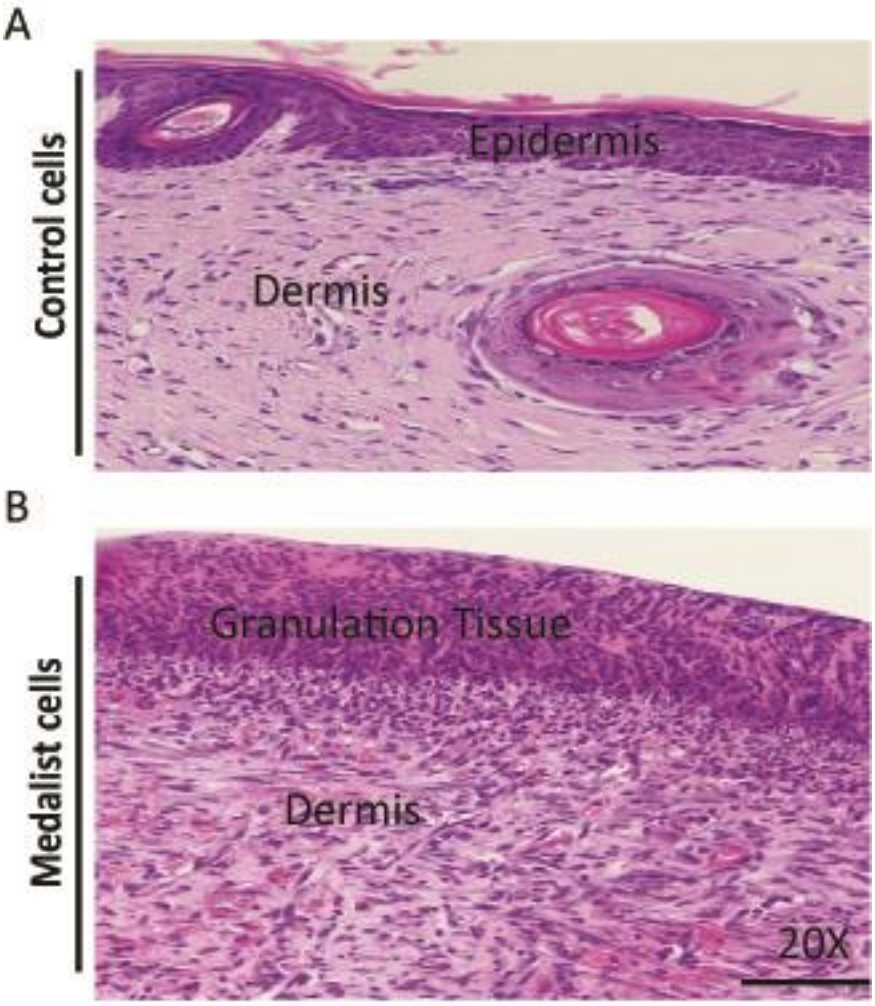

Supplemental Figure 14*:*
A high magnification pictures in H&E staining sections for completely healed (**A**) or open wound area and granulation tissues (**B**) at day 9 post-initial wounding. Scale bar: 161 mm.

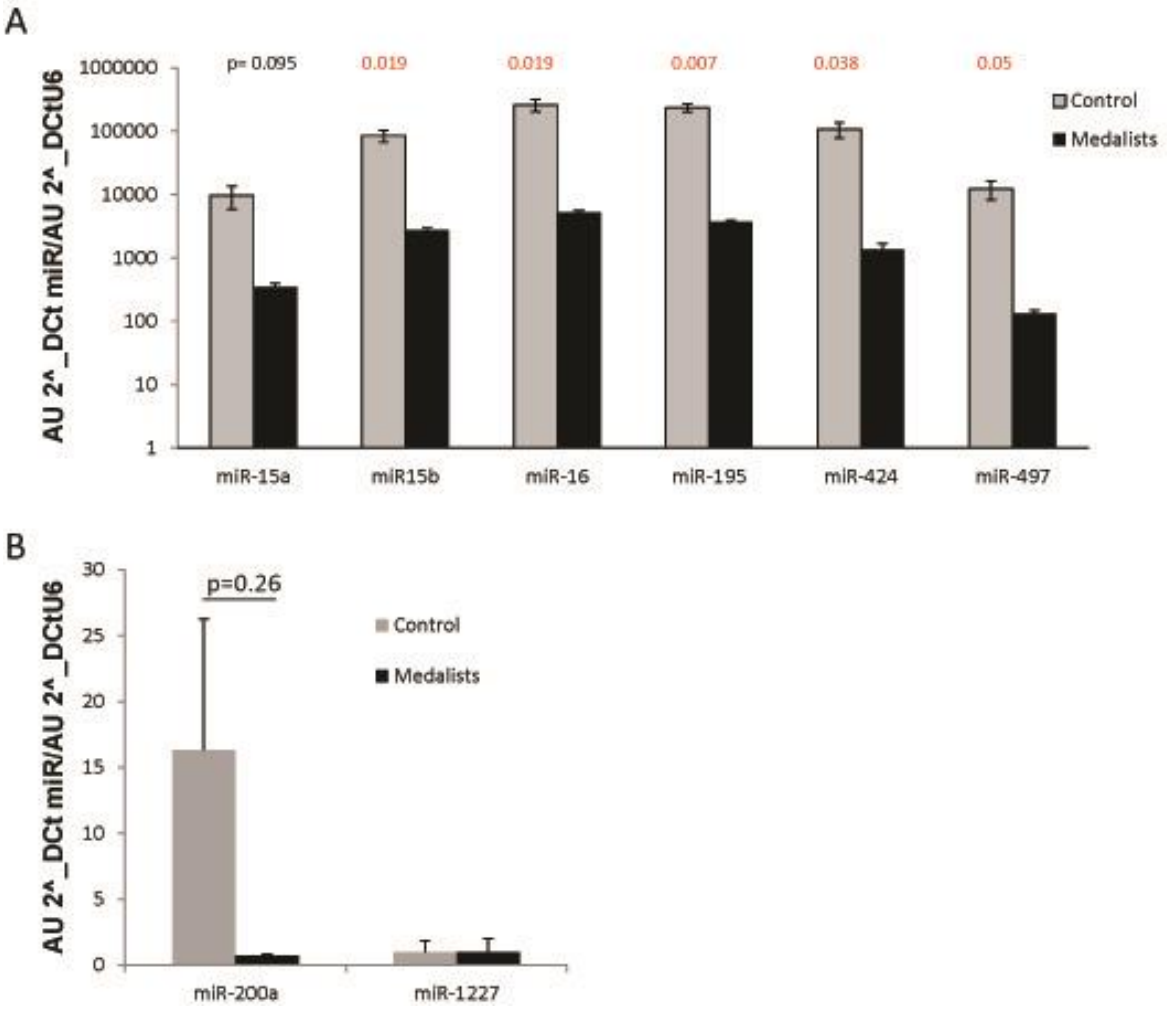

Supplemental Figure 15:
miRNA expression was studied in the Medalists' fibroblasts compared to the controls using qPCR analysis. The non-coding RNA U6 was used for normalization of miRNA qPCR results. Data are mean ± SD, n= 5 for both the control and the Medalist groups. The criteria for selecting the cell lines for these experiments were completely random, and the selected subjects did not differ in any clinical or demographic characteristics from the rest of the patients. Student's t-test or chi-square tests were used for two-way comparisons based on the distribution and number of observations of the variable.

Supplemental Table 1: **Cardiovascular disease characteristics of the 50-year Medalist cohort group**

Subjects with CVD

Donor	CAD	HA	number of HA	HWHA	number of HWHA	CABG	number of CABG	Angioplasty	number of Angiplasty	Leg bypass	Leg Angioplasty	number of LAA
1	Y	Y	1	Y	1	N	0	Y	1	N	N	0
2	Y	N	0	N	0	Y	2	Y	1	N	N	0
3	Y	Y	0	N	0	N	0	N	0	N	N	0
4	Y	Y	1	Y	1	Y	1	Y	1	Y	Y	1
5	Y	Y	2	Y	2	N	0	N	0	N	N	0
6	Y	Y	1	N	0	N	0	Y	2	N	N	0
7	Y	Y	3	Y	1	Y	1	Y	4	Y	Y	1
8	Y	Y	1	Y	1	Y	1	Y	1	Y	Y	1
9	Y	Y	1	N	0	N	0	N	0	Y	N	0
10	Y	Y	3	Y	3	Y	1	Y	1	N	Y	1
11	Y	Y	1	N	0	Y	1	Y	1	N	N	0
12	Y	N	0	N	0	Y	1	N	0	N	N	0
13	N	N	0	N	0	N	0	Y	2	N	N	0
14	N	N	0	N	0	N	0	N	0	N	Y	2
15	Y	Y	1	N	0	N	0	N	0	N	N	0
16	Y	Y	1	N	0	Y	1	N	0	N	N	0
17												
18	Y	Y	1	N	0	Y	1	N	0	N	N	0
	yes- 15	yes-13		yes-6		yes-9		yes-9		yes-4	yes-5	
	no-2	no-4		no-11		no-8		no-8		no-13	no-12	
	1 missing	1 missing	1 missing	1 missing	1 missing	1 missing	1 missing	1 missing	1 missing	1 missing	1 missing	1 missing

Subjects without CVD

19	N	N	0	N	0	N	0	N	0	N	N	0
20	N	N	0	N	0	N	0	N	0	N	N	0
21	N	N	0	N	0	N	0	N	0	N	N	0
22	N	N	0	N	0	N	0	N	0	N	N	0
23	N	N	0	N	0	N	0	N	0	N	N	0
24	N	N	0	N	0	N	0	N	0	N	N	0
25	N	N	0	N	0	N	0	N	0	N	N	0
26	N	N	0	N	0	N	0	N	0	N	N	0

CAD- Coronary Artery Disease; HA- Heart Attack; CABG- Coronary Artery Bypass Graft; HWHA- Hospitalization with Heart Attack. Y- yes; N-no.

Supplemental Table 2: Study subjects' clinical and demographic characteristics

		Age (yrs.)	Gender	Hemoglobin A1c (%)
1	Control	47	F	5.7
2	Control	49	M	5.9
3	Control	43	M	5.5
4	Control	47	F	5.9
5	T1D	56	F	9.5
6	T1D	66	F	7.2
7	T1D	52	M	5.6
8	T1D	62	M	9.2

F= female
M= male

Supplemental Table 3: Study subjects' demographics and clinical characteristics

		Age (yrs.)	Gender	Hemoglobin A1c (%)
1	**Control**	**53**	**M**	**N/A**
2	**Control**	**58**	**F**	**N/A**
3	**Control**	**65**	**F**	**N/A**
4	**Control**	**60**	**M**	**N/A**
5	**Control**	**56**	**F**	**N/A**
6	**DFU**	**57**	**M**	**11**
7	**DFU**	**63**	**M**	**11**
8	**DFU**	**52**	**M**	**N/D**
9	**DFU**	**50**	**F**	**N/D**
10	**DFU**	**52**	**F**	**8.5**
11	**DFU**	**57**	**M**	**9.5**

N/A = not applicable
N/D= not determined
F= female
M= male
DFU= diabetic foot ulcer

Supplemental Table 4: miRNAs might be predicted to bind to the 3'-UTR of the PKCδ mRNA in the Medalists and controls fibroblasts

	Predicted pairing of target region (top) and miRNA (bottom)	
Position 88-94 of PKCδ 3' UTR	5'	…GACUGUGGUGACUUCUGCUGCUG…
hsa-miR-15a	3'	….. GUGUUUGGUAAUACACGACGAU
hsa-miR-15b	3'	……ACAUUUGGUACUACACGACGAU
hsa-miR-16	3'	……GCGGUUAUAAAUGCACGACGAU
hsa-miR-195	3'	……..CGGUUAUAAAGACACGACGAU
hsa-miR-424	3'	…..AAGUUUUGUACUUAACGACGAC
hsa-miR-497	3'	…….UGUUUGGUGUCACACGACGAC

hsa= *Homo sapience*

Supplemental Table 5: **Sequences of the primers used for PCR**

Human VEGF	forward 5'-AGTCCAACATCACCATGCAG -3'	reverse 5'TTCCCTTTCCTCGAACTGATTT-3'
Human PDGF-BB	forward 5'GCAACAATTCCTGGCGATACC-3'	reverse 5'-CTCCACGGCTAACCACTG -3'
Human Fibronectin	forward 5'CAAGTATGAGAAGCCTGGGTCT -3'	reverse 5'-TGAAGATTGGGGTGTGGAAG-3'
Human PKCδ	forward 5'- AACGGGAGGTCTGCAGGG -3'	reverse 5'- TGCTTGTCCTTAGTCCTGGC-3'
Human 36B4	forward 5'-TGCTCAACATCTCCCCCTTCTC-3'	reverse 5'-ACCAAATCCCATATCCTCGTCC-3'
Human 18S ribosomal RNA	forward 5'- GTAACCCGTTGAACCCCATT-3'	reverse 5'-CCATCCAATCGGTAGTAGCG-3'
Human GAPDH	forward 5'-GCACCGTCAAGGCTGAGAAC-3'	Reverse 5'-GCCTTCTCCATGGTGGTGAA -3'